

3.4. In vivo antitumor activity of SMA–ZnPP

Based on the findings of pharmacokinetics of SMA–ZnPP described in Fig. 3, we first investigated the in vivo antitumor effect of SMA–ZnPP in rabbit VX-2 tumor model transplanted in the liver. As shown in Fig. 4 and Table 2, a remarkable antitumor effect of SMA–ZnPP was observed. At 40 days after tumor transplantation, all of the non-drug treated control tumor-bearing rabbits died, whereas all animals receiving SMA–ZnPP did survive (Table 2). On days 60 and 80 after VX-2 tumor inoculation, when SMA–ZnPP was given at 4 and 8 mg/kg (ZnPP equivalent, weekly injection for 4 weeks), the survival rate was 60% and 80%, respectively, whereas 12 mg/kg resulted 100% survival on day 80 (Table 2). More important, histological examination showed that tumors became necrotic and fibrosis after SMA–ZnPP treatment (Fig. 4). In a long-term study, out of seven animals treated with 7 mg/kg weekly for 4 weeks, four animals were cured with no recurrence of the tumor of up to 2 years period of follow-up.

Further, the antitumor activity of SMA–ZnPP was examined in a Meth A mouse fibrosarcoma model. As shown in Fig. 5A, tumor growth was remarkably suppressed when SMA–ZnPP was administered at the dose of 4 mg/kg. Growth suppression continued to at least for 19 days after injection of SMA–ZnPP.

Table 2

Therapeutic effect of SMA–ZnPP on rabbit VX-2 papiloma implanted in the liver.

Group	Dose (mg/kg) <sup>a</sup>	% Survival after treatment <sup>c</sup>			Histological changes (by laparotomy)
		40 days <sup>b</sup>	60 days <sup>b</sup>	80 days <sup>b</sup>	
Control	0	0	0	0	Growing with invasion
SMA–ZnPP	4	100	60	60	Fibrosis appearing
	8	100	80	80	Necrosis, fibrosis in tumors
	12	100	100	100	Necrosis, totally fibrosis

See text and Fig. 4 for details.

<sup>a</sup> ZnPP equivalent. SMA–ZnPP was injected once weekly for 4 weeks at the indicated doses.

<sup>b</sup> Days after tumor inoculation.

<sup>c</sup> n = 5–7 Per group.

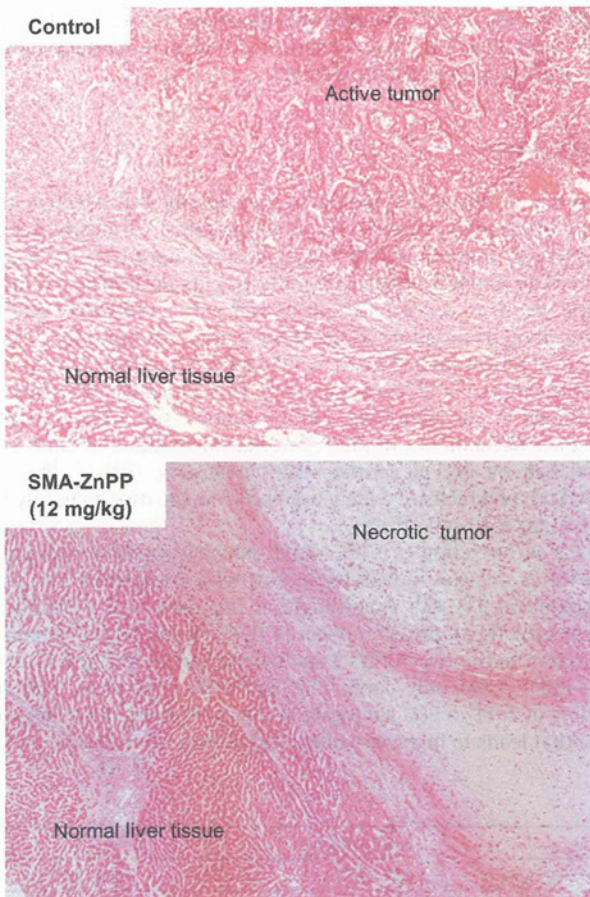


Fig. 4. Histological changes in rabbit VX-2 transplanted liver cancer after SMA–ZnPP treatment. Establishment of the tumor model is described in Materials and Methods. The dose of SMA–ZnPP was 12 mg/kg (ZnPP equivalent). Animals were killed, and tumor tissues were collected at 30 days (control group) and 60 days (SMA–ZnPP treatment group) after tumor inoculation, which were fixed by 10% buffered neutral formalin solution and were then subjected to H&E staining.

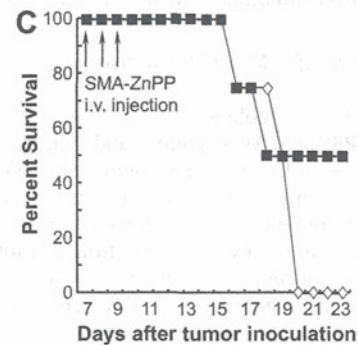
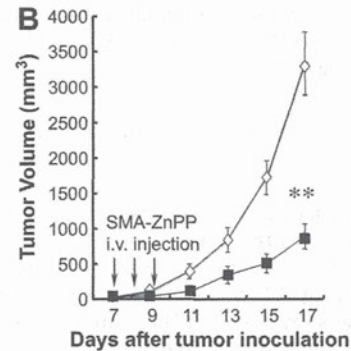
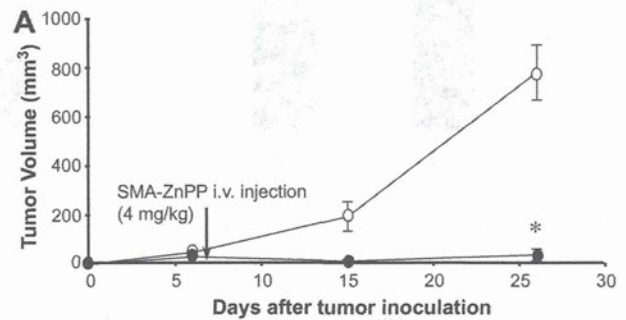
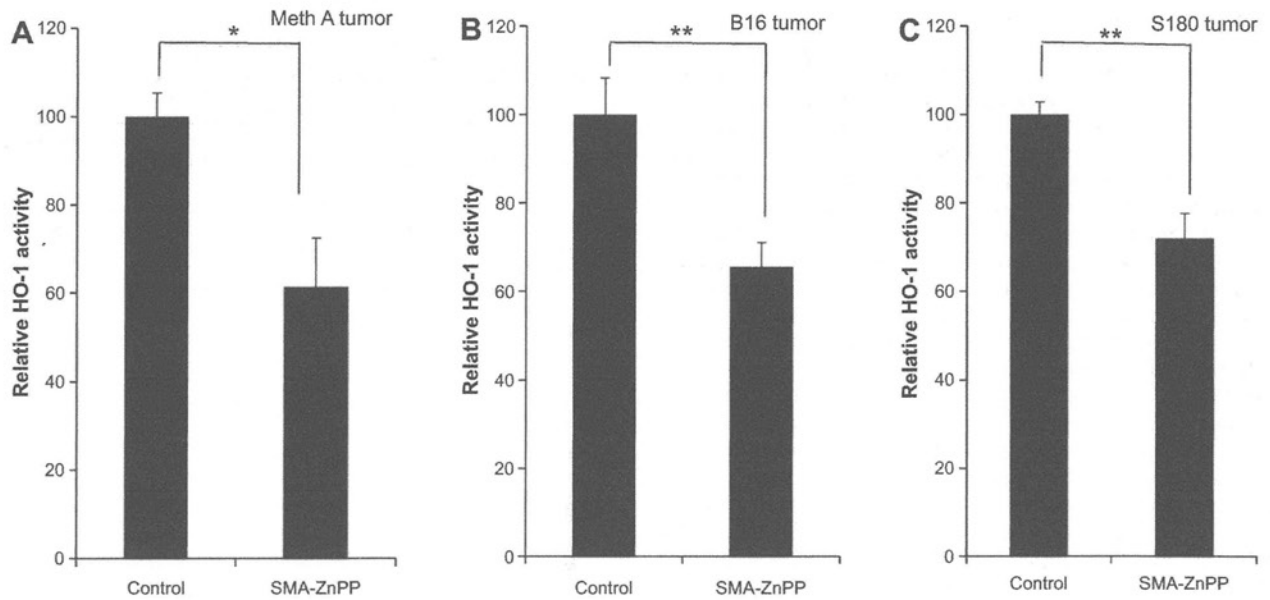


Fig. 5. In vivo antitumor effect of SMA–ZnPP. A shows the results in mouse MethA tumor model; ○, no drug control; ●, SMA–ZnPP (4 mg/kg ZnPP equivalent). B and C show the results of change in tumor size and survival of mouse B16 melanoma model; ◇, no drug control; ■, SMA–ZnPP (30 mg/kg ZnPP equivalent). Arrows indicate injections of SMA–ZnPP. Data are means (n = 6–8); bars, SE. \*P < 0.0001; \*\*P < 0.001, SMA–ZnPP treatment group vs untreated control group.

Similarly, in B16 melanoma in mice, which is known to progress rapidly and difficult to cure; significant suppression of tumor growth was found after 3 continuous injection of SMA–ZnPP at a



**Fig. 6.** Modulation by SMA-ZnPP of HO-1 activity in the Meth A (A), B16 (B) and S180 (C) solid tumor models. Tumor-bearing mice were i.v. injected with SMA-ZnPP (20 mg/kg, ZnPP equivalent). Twenty-four hours after the injection, tumors were obtained and were used for HO activity. Control mice values are means ( $n = 3-5$ ); bars, SE. \* $P < 0.01$ ; \*\* $P < 0.005$ , SMA-ZnPP treatment group vs untreated control group.

high dose (30 mg/kg) (Fig. 5B). Moreover, this treatment significantly contributed in the survival of tumor-bearing mice, that is, at 21 day after tumor inoculation, all mice of untreated control group died, whereas 50% of the mice in SMA-ZnPP treatment group remained alive (Fig. 5C).

### 3.5. Inhibition by SMA-ZnPP of HO activity in Meth A and B16 solid tumor

To clarify whether the *in vivo* suppression of tumor growth by SMA-ZnPP was due to the inhibition of HO activity, the enzyme activity of HO-1 in tumor after SMA-ZnPP treatment was examined. As shown in Fig. 6, HO-1 activity was significantly suppressed in all tested tumors (by 30–40%). These findings support our working hypothesis of the antitumor mechanisms of SMA-ZnPP, that is, through the HO-1 inhibition pathway, at least partly.

### 3.6. Adverse effect of SMA-ZnPP treatment

As summarized in Table 3, no significant adverse effects such as decreases in RBC and WBC counts and hemoglobin levels were found 72 h after SMA-ZnPP treatment at the dose of 50 mg/kg, which is much higher than the therapeutic dose or effective dose. Also, no significant changes in the liver enzymes and kidney functions were found under the same conditions (Table 3).

In addition, in a long-term follow-up of the above SMA-ZnPP treatment at high dose by a bolus administration (200 mg/kg), no

death or body weight changes was observed up to 3 months after SMA-ZnPP injection (data not shown). These data strongly suggest the safety of SMA-ZnPP treatment.

## 4. Discussions

In this study, we demonstrated the superior and selective anti-tumor effect of SMA-ZnPP, both *in vitro* against various tumor cell lines (Fig. 1, Table 1), and *in vivo* against different type of solid tumors (Figs. 4 and 5), especially indicating its potential as a therapeutic for liver cancer. The antitumor activity of SMA-ZnPP is achieved by its targeting to the HO-1 that is a important "survival factor" of most tumors [2,5,6], which ZnPP is the pharmacological active principle to inhibit HO-1 activity. This anticancer strategy was developed in our laboratory, and to improve the water-solubility and pharmacokinetics of ZnPP, micellar formations of ZnPP were developed by use of various water polymers, that is, PEG and SMA, both of which are widely used polymers to modify hardly soluble small molecular drugs.

One of the examples is PEG-ZnPP, which is a polymer conjugate that forms micelles in water solutions with superior *in vivo* pharmacokinetics [12,13]. Accordingly, it demonstrated a significant tumor growth suppression effect [13]. However, we have found a limitation to the use of PEG as polymeric carrier of ZnPP. Namely, PEG-ZnPP could only carry 1.5% ZnPP/PEG w/w ratio. This low loading of ZnPP in PEG conjugate requires relatively large injection dose that leads to high viscosity at higher dose that may be needed

**Table 3**  
Effect of SMA-ZnPP in hematology and liver, kidney function.<sup>a</sup>

	Hematological findings			Kidney function		Liver enzymes		
	RBC ( $10^4/\mu\text{l}$ )	WBC ( $/\mu\text{l}$ )	Hb (g/l)	BUN (mg/dl)	Cr (mg/dl)	AST (IU/l)	ALT (IU/l)	LDH (IU/l)
Control	868.7 ± 60.6	186.7 ± 18.8	13.4 ± 1.2	23.0 ± 0.6	0.11 ± 0.01	395.3 ± 91.8	26.0 ± 3.8	10697.5 ± 2247.6
SMA-ZnPP <sup>b</sup>	820.0 ± 70.5	206.5 ± 52.0	2.3 ± 1.2	25.9 ± 1.1	0.13 ± 0.01	351.8 ± 88.9	27.5 ± 2.7	9755.0 ± 1570.8

Abbreviations used are: Hb, hemoglobin; BUN, blood urea nitrogen; Cr, creatinine; AST, aspartate aminotransferase; ALT, alanine aminotransferase; LDH, lactate dehydrogenase.

<sup>a</sup> No significant difference was found between SMA-ZnPP treatment group and control group in all selected indices. Values are presented as means ± SE.

<sup>b</sup> SMA-ZnPP was administered *i.v.* at 50 mg/kg (ZnPP equivalent). Assays were carried out at 72 h after SMA-ZnPP treatment.

for possible human therapeutic application. Further, the cost of expensive PEG for such low loading drug results in relatively high drug cost, which will become a social problem. To overcome these drawbacks, we further developed a micellar type of ZnPP using SMA, namely SMA-ZnPP, which can achieve higher loading of 15–45% w/w [14]. The high loading did not affect its solubility in this micelle; on the contrary, it resulted in solubility of up to 150 mg/ml, which can exceed the solubility required for therapeutic application.

In addition to the increased water-solubility, SMA-ZnPP also showed faster cellular uptake in all three different tumor cell lines tested, which is comparable to that of free ZnPP. Namely, it was about three times higher than PEG-ZnPP (Fig. 2). In our recent report, we compared the intracellular fate of free ZnPP and its polymer conjugates and micells (i.e., SMA-ZnPP and PEG-ZnPP) [17]. While free ZnPP was taken up via free diffusion, SMA-ZnPP was mostly internalized by endocytosis. During this internalization process, the micelle integrity was disrupted and free ZnPP appeared to be released upon internalization with cell membrane components [17]. However, the intracellular uptake of PEG-ZnPP was greatly impeded, which is called PEG dilemma [17,18]. The data in present study are consistent with our previous findings, suggesting that SMA-ZnPP shows stronger cytotoxicity than PEG-ZnPP because of its efficient cell uptake. To verify this notion, we tested the cytotoxicity of SMA-ZnPP in various tumor cells, which exhibited a mean  $IC_{50}$  of 11.1  $\mu$ M (Table 1), whereas as reported previously, PEG-ZnPP showed a relatively higher  $IC_{50}$  of about 20  $\mu$ M [13].

SMA-ZnPP micelle appeared as large molecule with the apparent molecular size of 144 kDa as determined by size exclusion chromatography [14]. As such large molecule, we thus anticipated its higher intratumor concentration based on the EPR effect followed by rapid endocytosis. It appears to be an universal phenomenon of macromolecular drugs with molecular weight larger than 40 kDa, a feature of the EPR effect, which they are selectively accumulated and being retained in solid tumor because of the unique anatomical and pathophysiological characteristics of tumor vasculature [19], and it is now known as a gold standard for the design and development of anticancer drugs [20–26].

However, we could not find good EPR effect for SMA-ZnPP in the present study, even though it showed stable macromolecular micellar structure in physiological solution as described in our previous report [14]. This may be probably due to the lack of *in vivo* stability particularly in circulation, namely SMA-ZnPP micelle may be disrupted during circulation or upon uptake by RES which are rich in liver and spleen. Because of the high affinity to liver and spleen, free ZnPP released from SMA-ZnPP after disruption will accumulate mostly in liver and spleen. In consistent with this notion, we found interestingly that SMA-ZnPP significantly accumulated in liver tissue, for example, 20 times higher than plasma concentration at 24 h after *i.v.* injection, and it retained in the liver tissue at relatively high concentration for more than 96 h (Fig. 3C). The disruption and high liver accumulation of SMA-ZnPP could be improved by conjugation of SMA with ZnPP via a covalent amide bond (unpublished data). These data of distribution study, however, strongly suggest us to use SMA-ZnPP for the treatment of the liver cancer that is very difficult to treat in clinic with high mortality. Accordingly, in the present study, a significant cure rate of rabbits with VX-2 tumor implanted in the liver was achieved by using SMA-ZnPP, evidences being not only by the survival rate of animals, but also by the histopathological examination, that is, SMA-ZnPP treatment resulted in more necrosis as well as fibrosis of tumor tissues (Fig. 4 and Table 2).

Moreover, in other tumor models, that is, Meth A and B16 melanoma, SMA-ZnPP markedly reduced the tumor volume (Fig. 5), though complete regression of the tumor was not possible in B16

melanoma as in VX-2. In addition, compared to B16 tumors, Meth A tumors showed higher sensitivity to this treatment. Namely, a lower dose of SMA-ZnPP (at 4 mg/kg bolus *i.v.*) exhibited relatively remarkable tumor suppression effect (Fig. 5A) compared to B16 tumor with higher dose treatment of SMA-ZnPP (three injections of 30 mg/kg) (Fig. 5B). These findings are consistent with the cytotoxicity data of these two cell lines ( $IC_{50}$  of Meth A, 10.8  $\mu$ M vs 20.1  $\mu$ M of B16, Table 1).

The antitumor mechanisms of SMA-ZnPP were considered mostly due to the HO-1 inhibition activity, and variation of HO-1 dependence susceptibility in different tumors may result in the variation of therapeutic effect. This notion was partly verified in the present study, namely, SMA-ZnPP treatment decreased the HO-1 activity in Meth A, B16 and S180 solid tumors, significantly though not largely (Fig. 6). It should be also noted that many other possible mechanisms may also work for the antitumor activity of SMA-ZnPP. For example, it has been reported that ZnPP-induced apoptosis of hamster fibroblasts by upregulating p53 expression, through ZnPP-mediated Egr-1 binding [27]. More recently, down-regulation of BCR/ABL oncogene by ZnPP in case of chronic myeloid leukemia (CML) has been reported [28]. Administration of PEG-ZnPP or SMA-ZnPP showed a remarkable therapeutic potential against CML [29,30], even imatinib-resistant CML [31]. In addition, SMA copolymer itself was found to have an active role in endogenous interferon induction as well as the activation of NK cells [32–34]. Furthermore, zinc is also known as an essential messenger molecule in stimulating immune response [35], and it was also used for the treatment of prostate cancer, probably via a mitochondrial-mediated apoptotic pathway [36–38]; it thus may serve as another mechanism of SMA-ZnPP-induced antitumor effect by releasing zinc from the porphyrin ring of ZnPP. The roles of various factors in mediating different anticancer activity of SMA-ZnPP in tumors, however, remain to be investigated.

Even though SMA-ZnPP accumulated predominantly in the liver tissues, we did not find apparent adverse effects during our experiments. In addition, no deterioration of the liver functions was observed even at high dose of SMA-ZnPP (50 mg/kg) (Table 3). This may be, at least partly, due to the differences of sensitivities to SMA-ZnPP between normal and tumor cells. This notion was supported by *in vitro* MTT assay, which showed a relatively strong cytotoxicity of SMA-ZnPP against various tumor cells (Table 1), that is, the  $IC_{50}$  of SMA-ZnPP to human liver cancer cells Sk-Hep was 16  $\mu$ M, and the range of  $IC_{50}$  in different tumor cells was between 3 and 20  $\mu$ M. Importantly and interestingly, normal cells seemed to be much tolerant to SMA-ZnPP. Namely, the  $IC_{50}$  of SMA-ZnPP to normal hepatocytes Hc was higher than 50  $\mu$ M, as well as other normal cells (Table 1). The difference of the responses of tumor cells and normal cells against SMA-ZnPP treatment may be due to the difference of HO-1 expression between tumor and normal cells, as described earlier [2,5,6,13]; however, further investigations are needed to define this correlation.

SMA-ZnPP used in our animal study, with some exceptions, was at the dose range of 1–10 mg/kg; however, animals were able to tolerate as high as 50 mg/kg without any apparent toxicity as reflected by blood cells count and biochemical examination of liver and kidney functions (Table 3), as well as survival rate. These data indicate the high safety of SMA-ZnPP with a wide therapeutic window.

## 5. Conclusions

The water-soluble micellar type of HO-1 inhibitor SMA-ZnPP was found to be effective in many solid tumor models, especially VX-2 tumor transplanted in the liver of rabbit. The drug accumulated in the liver was very high, while clearance from the circula-

tion was relatively rapid. SMA–ZnPP was examined both in vitro and in vivo; whereas it showed relatively potent cytotoxicity to tumor cells (average  $IC_{50}$  of about 11  $\mu$ M); the  $IC_{50}$  of normal cells was higher than 50  $\mu$ M, which resulted in very little adverse effects to tumor-bearing animals. These findings suggest the potential use of SMA–ZnPP as a novel anticancer drug especially for liver cancer, which warrants further development and investigation.

### Acknowledgment

The authors wish to thank Dr. Takahiro Seki for excellent technical assistance.

### Appendix A. Supplementary material

Supplementary data associated with this article can be found, in the online version, at <http://dx.doi.org/10.1016/j.ejpb.2012.04.016>.

### References

- [1] M.D. Maines, Heme oxygenase: function, multiplicity, regulatory mechanisms, and clinical applications, *FASEB J.* 2 (1988) 2257–2268.
- [2] J. Fang, T. Akaike, H. Maeda, Antiapoptotic role of heme oxygenase (HO) and the potential of HO as a target in anticancer treatment, *Apoptosis* 9 (2004) 27–35.
- [3] S.M. Keyse, R.M. Tyrrell, Heme oxygenase is the major 32-kDa stress protein induced in human skin fibroblasts by UVA radiation, hydrogen peroxide, and sodium arsenite, *Proc. Natl. Acad. Sci. USA* 86 (1989) 99–103.
- [4] R. Motterlini, R. Foresti, R. Bassi, B. Calabrese, J.E. Clark, C.J. Green, Endothelial heme oxygenase-1 induction by hypoxia. Modulation by inducible nitric oxide synthase and S-nitrosothiols, *J. Biol. Chem.* 275 (2000) 13613–13620.
- [5] K. Doi, T. Akaike, S. Fujii, S. Tanaka, N. Ikebe, T. Beppu, S. Shibahara, M. Ogawa, H. Maeda, Induction of haem oxygenase-1 by nitric oxide and ischaemia in experimental solid tumours and implications for tumour growth, *Br. J. Cancer* 80 (1999) 1945–1954.
- [6] S. Tanaka, T. Akaike, J. Fang, T. Beppu, M. Ogawa, F. Tamura, Y. Miyamoto, H. Maeda, Antiapoptotic effect of haem oxygenase-1 induced by nitric oxide in experimental solid tumour, *Br. J. Cancer* 88 (2003) 902–909.
- [7] J.P. Greenstein, *Biochemistry of Cancer*, second ed., Academic Press, New York, 1954.
- [8] Y. Hasegawa, T. Takano, A. Miyauchi, F. Matsuzaka, H. Yoshida, K. Kuma, N. Amino, Decreased expression of glutathione peroxidase mRNA in thyroid anaplastic carcinoma, *Cancer Lett.* 182 (2002) 69–74.
- [9] N. Yamanaka, D. Deamer, Superoxide dismutase activity in WI-38 cell cultures: effect of age, trypsinization and SV-40 transformation, *Physiol. Chem. Phys.* 6 (1974) 95–106.
- [10] K. Sato, K. Ito, H. Kohara, Y. Yamaguchi, K. Adachi, H. Endo, Negative regulation of catalase gene expression in hepatoma cells, *Mol. Cell. Biol.* 12 (1992) 2525–2533.
- [11] J. Fang, D. Deng, H. Nakamura, T. Akuta, H. Qin, A.K. Iyer, K. Greish, H. Maeda, Oxystress inducing antitumor therapeutics via tumor-targeted delivery of PEG-conjugated D-amino acid oxidase, *Int. J. Cancer* 122 (2008) 1135–1144.
- [12] S.K. Sahoo, T. Sawa, J. Fang, S. Tanaka, Y. Miyamoto, T. Akaike, H. Maeda, Pegylated zinc protoporphyrin: a water-soluble heme oxygenase inhibitor with tumor-targeting capacity, *Bioconjug. Chem.* 13 (2002) 1031–1038.
- [13] J. Fang, T. Sawa, T. Akaike, T. Akuta, S.K. Sahoo, G. Khaled, A. Hamada, H. Maeda, In vivo antitumor activity of pegylated zinc protoporphyrin: targeted inhibition of heme oxygenase in solid tumor, *Cancer Res.* 63 (2003) 3567–3574.
- [14] A.K. Iyer, K. Greish, J. Fang, R. Murakami, H. Maeda, High-loading nanosized micelles of copoly(styrene-maleic acid)-zinc protoporphyrin for targeted delivery of a potent heme oxygenase inhibitor, *Biomaterials* 28 (2007) 1871–1881.
- [15] A. Kobayashi, T. Oda, H. Maeda, Protein binding of macromolecular anticancer agent SMANCS: characterization of poly(styrene-co-maleic acid) derivatives as an albumin binding ligand, *J. Bioact. Compat. Polym.* 3 (1988) 319–333.
- [16] K. Greish, A. Nagamitsu, J. Fang, H. Maeda, Copoly(styrene-maleic acid)-pirarubicin micelles: high tumor-targeting efficiency with little toxicity, *Bioconjug. Chem.* 16 (2005) 230–236.
- [17] H. Nakamura, J. Fang, B. Gahininath, K. Tsukigawa, H. Maeda, Intracellular uptake and behavior of two types zinc protoporphyrin (ZnPP) micelles, SMA–ZnPP and PEG–ZnPP as anticancer agents; unique intracellular disintegration of SMA micelles, *J. Control. Release* 155 (2011) 367–375.
- [18] H. Hatakeyama, H. Akita, H. Harashima, A multifunctional envelope type nano device (MEND) for gene delivery to tumours based on the EPR effect: a strategy for overcoming the PEG dilemma, *Adv. Drug Deliv. Rev.* 63 (2011) 152–160.
- [19] Y. Matsumura, H. Maeda, A new concept for macromolecular therapeutics in cancer chemotherapy: mechanism of tumoritropic accumulation of proteins and the antitumor agent SMANCS, *Cancer Res.* 46 (1986) 6387–6392.
- [20] H. Maeda, T. Sawa, T. Konno, Mechanism of tumor-targeted delivery of macromolecular drugs, including the EPR effect in solid tumor and clinical overview of the prototype polymeric drug SMANCS, *J. Control. Release* 74 (2001) 47–61.
- [21] K. Greish, J. Fang, T. Inutsuka, A. Nagamitsu, H. Maeda, Macromolecular therapeutics: advantages and prospects with special emphasis on solid tumour targeting, *Clin. Pharmacokinet.* 42 (2003) 1089–1105.
- [22] H. Maeda, Tumor-selective delivery of macromolecular drugs via the EPR effect: background and future prospects, *Bioconjug. Chem.* 21 (2010) 797–802.
- [23] R. Duncan, The dawning era of polymer therapeutics, *Nat. Rev. Drug Discov.* 2 (2003) 347–360.
- [24] H. Maeda, G.Y. Bharate, J. Daruwala, Polymeric drugs for efficient tumor-targeted drug delivery based on EPR-effect, *Eur. J. Pharm. Biopharm.* 71 (2009) 409–419.
- [25] T. Seki, J. Fang, H. Maeda, Tumor targeted macromolecular drug delivery based on the enhanced permeability and retention effect in solid tumor, in: Y. Lu, R.I. Mahato (Eds.), *Pharmaceutical Perspectives of Cancer Therapeutics*, AAPS-Springer Publishing, New York, 2009, pp. 93–102.
- [26] J. Fang, H. Nakamura, H. Maeda, The EPR effect: unique features of tumor blood vessels for drug delivery, factors involved, and limitations and augmentation of the effect, *Adv. Drug Deliv. Rev.* 63 (2010) 136–151.
- [27] G. Yang, X. Nguyen, J. Qu, P. Rekulapelli, D.K. Stevenson, P.A. Dennery, Unique effects of zinc protoporphyrin on HO-1 induction and apoptosis, *Blood* 97 (2001) 1306–1313.
- [28] M. Mayerhofer, S. Florian, M.T. Krauth, K.J. Aichberger, M. Bilban, R. Marculescu, D. Printz, G. Fritsch, O. Wagner, E. Selzer, W.R. Sperr, P. Valent, C. Sillaber, Identification of heme oxygenase-1 as a novel BCR/ABL-dependent survival factor in chronic myeloid leukemia, *Cancer Res.* 64 (2004) 3148–3154.
- [29] R. Kondo, K.V. Gleixner, M. Mayerhofer, A. Vales, A. Gruze, P. Samorapompichit, K. Greish, M.T. Krauth, K.J. Aichberger, W.F. Pickl, H. Esterbauer, C. Sillaber, H. Maeda, P. Valent, Identification of heat shock protein 32 (Hsp32) as a novel survival factor and therapeutic target in neoplastic mast cells, *Blood* 110 (2007) 661–669.
- [30] E. Hadzjuszufovic, L. Rebuzzi, K.V. Gleixner, V. Ferenc, B. Peter, R. Kondo, A. Gruze, M. Kneidinger, M.T. Krauth, M. Mayerhofer, P. Samorapompichit, K. Greish, A.K. Iyer, W.F. Pickl, H. Maeda, M. Willmann, P. Valent, Targeting of heat-shock protein 32/heme oxygenase-1 in canine mastocytoma cells is associated with reduced growth and induction of apoptosis, *Exp. Hematol.* 36 (2008) 1461–1470.
- [31] M. Mayerhofer, K.V. Gleixner, J. Mayerhofer, G. Hoermann, E. Jaeger, K.J. Aichberger, R.G. Ott, K. Greish, H. Nakamura, S. Derdak, P. Samorapompichit, W.F. Pickl, V. Sexl, H. Esterbauer, I. Schwarzingler, C. Sillaber, H. Maeda, P. Valent, Targeting of heat shock protein 32 (Hsp32)/heme oxygenase-1 (HO-1) in leukemic cells in chronic myeloid leukemia: a novel approach to overcome resistance against imatinib, *Blood* 111 (2008) 2200–2210.
- [32] F. Suzuki, R.B. Pollard, S. Uchimura, T. Munakata, H. Maeda, Role of natural killer cells and macrophages in the nonspecific resistance to tumors in mice stimulated with SMANCS, a polymer-conjugated derivative of neocarzinostatin, *Cancer Res.* 50 (1990) 3897–3904.
- [33] F. Suzuki, T. Munakata, H. Maeda, Interferon induction by SMANCS: a polymer-conjugated derivative of neocarzinostatin, *Anticancer Res.* 8 (1988) 97–103.
- [34] T. Oda, T. Morinaga, H. Maeda, Stimulation of macrophage by polyanions and its conjugated proteins and effect on cell membrane, *Proc. Soc. Exp. Biol. Med.* 181 (1986) 9–17.
- [35] H. Haase, J.L. Ober-Blöbaum, G. Engelhardt, S. Hebel, A. Heit, H. Heine, L. Rink, Zinc signals are essential for lipopolysaccharide-induced signal transduction in monocytes, *J. Immunol.* 181 (2008) 6491–6502.
- [36] L.C. Costello, R.B. Franklin, P. Feng, Mitochondrial function, zinc, and intermediary metabolism relationships in normal prostate and prostate cancer, *Mitochondrion* 5 (2005) 143–153.
- [37] P. Feng, T. Li, Z. Guan, R.B. Franklin, L.C. Costello, The involvement of Bax in zinc-induced mitochondrial apoptosis in malignant prostate cells, *Mol. Cancer* 7 (2008) 25.
- [38] S.F. Lin, H. Wei, D. Maeder, R.B. Franklin, P. Feng, Profiling of zinc-altered gene expression in human prostate normal vs. cancer cells: a time course study, *J. Nutr. Biochem.* 20 (2009) 1000–1012.

## PEGylated D-amino acid oxidase restores bactericidal activity of neutrophils in chronic granulomatous disease via hypochlorite

Hideaki Nakamura<sup>1,2</sup>, Jun Fang<sup>1,2</sup>, Tomoyuki Mizukami<sup>3</sup>, Hiroyuki Nuno<sup>4</sup> and Hiroshi Maeda<sup>2</sup>

<sup>1</sup>Laboratory of Microbiology and Oncology, Faculty of Pharmaceutical Science; <sup>2</sup>Institute for Drug Delivery System Research, Sojo University, Ikeda 4-22-1, Kumamoto 860-0082; <sup>3</sup>Department of Pediatrics, Kumamoto Saishunsou National Hospital, 2659 Suya, Kohshi, Kumamoto 861-1196; <sup>4</sup>Division of Pediatrics, Department of Reproductive and Developmental Medicine, Faculty of Medicine, University of Miyazaki, Kiyotake-cho, Kihara 5200, Miyazaki 889-1692, Japan  
Corresponding author: Hiroshi Maeda. Email: hirmaeda@ph.sojo-u.ac.jp

### Abstract

Chronic granulomatous disease (CGD) causes impaired hydrogen peroxide (H<sub>2</sub>O<sub>2</sub>) generation. Consequently, neutrophils in patients with CGD fail to kill infecting pathogens. We expected that supplementation with H<sub>2</sub>O<sub>2</sub> would effectively restore the bactericidal function of neutrophils in CGD. Here, we used polyethylene glycol-conjugated D-amino acid oxidase (PEG-DAO) as an H<sub>2</sub>O<sub>2</sub> source. The enzyme DAO generates H<sub>2</sub>O<sub>2</sub> by using D-amino acid and oxygen as substrates. PEG-DAO plus D-amino acid indeed exerted bacteriostatic activity against *Staphylococcus aureus* via H<sub>2</sub>O<sub>2</sub> *in vitro*. Furthermore, use of PEG-DAO plus D-amino acids, which increased the amount of intracellular H<sub>2</sub>O<sub>2</sub>, restored bactericidal activity of neutrophils treated with diphenylene iodonium, in which nicotinamide adenine dinucleotide phosphate (NADPH) oxidase was defective. This restoration of bactericidal activity was mediated by myeloperoxidase, with concomitant production of H<sub>2</sub>O<sub>2</sub> by PEG-DAO plus D-Ala. We also confirmed that PEG-DAO treatment restored bactericidal activity of congenitally defective neutrophils from patients with CGD. These results indicate that PEG-DAO can supply additional H<sub>2</sub>O<sub>2</sub> for defective NADPH oxidase of neutrophils from patients with CGD, and thus neutrophils regain bactericidal activity.

**Keywords:** PEG-DAO, chronic granulomatous disease, hydrogen peroxide, H<sub>2</sub>O<sub>2</sub> supplementation therapy

*Experimental Biology and Medicine* 2012; **237**: 703–708. DOI: 10.1258/ebm.2012.011360

### Introduction

Chronic granulomatous disease (CGD) is a genetic disorder characterized by chronic and recurrent pyogenic infections. Patients with CGD have a defect in nicotinamide adenine dinucleotide phosphate (NADPH) oxidase that results in dysfunctional production of hydrogen peroxide (H<sub>2</sub>O<sub>2</sub>).<sup>1,2</sup> H<sub>2</sub>O<sub>2</sub> plays a pivotal role in the antibacterial function of neutrophils, mediated by myeloperoxidase (MPO), so the impaired H<sub>2</sub>O<sub>2</sub> production means failure of bactericidal activity against pathogenic organisms such as *Staphylococcus aureus*.<sup>2,3</sup>

D-Amino acid oxidase (DAO) is an enzyme containing flavin adenine dinucleotide (FAD).<sup>4</sup> The biochemical function of DAO involves oxidative deamination of D-amino acids, which yields the corresponding  $\alpha$ -keto acids, a process in which molecular oxygen is used as an electron acceptor and H<sub>2</sub>O<sub>2</sub> is generated.<sup>5</sup>

We previously prepared polyethylene glycol (PEG)-conjugated DAO (PEG-DAO) with comparable enzyme activity to native DAO.<sup>6,7</sup> More importantly, PEG-DAO had a longer circulation time in the blood, and preferential

accumulation in inflamed sites, as a result of the enhanced permeability and retention (EPR) effect.<sup>8,9</sup> Our previous report showed that PEG-DAO exhibited selective cytotoxicity against various cancer cells via production of H<sub>2</sub>O<sub>2</sub> *in vivo* and *in vitro*.<sup>6,7</sup>

We therefore anticipated that PEG-DAO would function as an alternative supplier of H<sub>2</sub>O<sub>2</sub> for neutrophils in patients with CGD. In this study, we therefore investigated the effect of PEG-DAO on bactericidal activity of neutrophils from mice in which NADPH oxidase was inhibited, and from a patient with CGD, and analyzed the mechanism of bactericidal activity, in addition to investigating MPO-inhibited neutrophils.

### Materials and methods

#### Materials

*S. aureus* strain ATCC25923 was used in these studies. ICR mice were purchased from Japan SLC, Inc., Shizuoka,

Japan. Trypticase soy (SCD) broth was purchased from Nissui Seiyaku Co., Tokyo, Japan. Flavin adenine dinucleotide was purchased from Sigma-Aldrich Chemical Co. (St Louis, MO, USA). Trypticase soy agar, isopropyl- $\beta$ -D-thiogalactopyranoside, carbenicillin, Tween-20, ammonium sulfate, casein sodium salt and other reagents were from Wako Pure Chemical Industries, Ltd, Osaka, Japan. 4-aminobenzoic acid hydrazide (4-ABH) was from Merck KGaA, Frankfurt, Germany. Diphenylene iodonium (DPI) was purchased from Tokyo Chemical Industry Co., Ltd, Tokyo, Japan. Succinimide-activated PEG (MEC-50HS), with an average molecular size of Mr 5000, was purchased from Nippon Oil & Fat Co. (Tokyo, Japan).

### Preparation of PEG-DAO

Recombinant porcine DAO was prepared as described previously.<sup>7</sup> Briefly, *Escherichia coli* BL21 (DE3) bacteria harboring the pET3c plasmid encoding porcine DAO were cultured in LB medium containing 50  $\mu$ g/mL carbenicillin, and porcine DAO expression was achieved by adding 10  $\mu$ mol/L isopropyl- $\beta$ -D-thiogalactopyranoside to the medium with *E. coli*. After culture of the bacteria at 37°C for 20 h, bacterial pellets were sonicated (150 W, 30 min) in 17 mmol/L pyrophosphate buffer (pH 8.2), and porcine DAO was obtained by heat denaturation at 59°C for three minutes, followed by ammonium sulfate precipitation at 35% saturation, and then diethylaminoethyl cellulose column chromatography ( $L = 10$  cm  $\times$   $\phi = 1.6$  cm). The purity of DAO (>90%) was determined by using sodium dodecylsulfate polyacrylamide gel electrophoresis after staining with Coomassie brilliant blue. PEGylation of DAO was conducted as described previously.<sup>6</sup> In brief, to the DAO solution (2.0 mg/mL protein in 50 mmol/L sodium phosphate buffer, pH 7.4), succinimide-activated PEG was added at a 3.5 mol/L excess of PEG/mol of free amino groups in DAO and was allowed to react for one hour at 4°C. The reaction mixture containing PEG-DAO thus obtained was then purified to remove free PEG and other low-molecular-weight reactants by ultrafiltration with the YM-10 membrane (Millipore) using 10 times the volume of 10 mmol/L phosphate-buffered saline (PBS). PEG-DAO was stored in PBS containing 0.1 mmol/L FAD at 4°C. Approximately 30% of the amino groups on DAO was reacted with PEG.

### Bacteriostatic assay

*S. aureus* bacteria were cultured until the mid-log phase of growth in SCD broth with reciprocal shaking at 37°C. *S. aureus* were washed twice in saline and  $1 \times 10^5$  CFU/mL of *S. aureus* were incubated with various concentrations of PEG-DAO, D-Ala, and with or without catalase in SCD broth at 37°C for five hours. The relative total numbers of bacteria were measured at turbidity at 570 nm and were correlated with the numbers of viable bacteria.

### Preparation of neutrophils

Peritoneal neutrophils were elicited in 10-week-old female ICR mice by intraperitoneal injection of 3 mL per mouse of 6% casein sodium salt dissolved in physiological saline. At six hours after injection, neutrophils were harvested via peritoneal lavage with 5 mL of PBS, pH 7.4. Contaminating erythrocytes were removed by incubating in hypotonic saline solution (0.2% NaCl) for 30 s to cause erythrocytes to burst, after which isotonicity was restored via a rebalancing solution (1.9% NaCl) followed by centrifugation. Approximately  $1 \times 10^7$  neutrophils were obtained from 10-week-old female ICR mice. The purity of the neutrophils (>90%) was checked by using Giemsa staining and examination of cell morphology with a conventional microscope (ECLIPSE TS100; Nikon, Tokyo, Japan). Human peripheral neutrophils were collected from a patient with CGD and a healthy volunteer using Polymorphprep™ (Cosmo Bio, Tokyo, Japan) according to the manufacturer's instruction. Briefly, 5 mL of human blood sample was carefully layered on the top of 5 mL of Polymorphprep™, followed by centrifugation with a swing-out rotor for 30 min at  $450 \times g$ . The neutrophil fraction was collected and mixed with 0.45% NaCl, and then centrifuged for 10 min at  $400 \times g$ . Neutrophil pellets were then resuspended in PBS (-) and used for further experiments.

### Bactericidal activity of neutrophils and preparation of CGD neutrophil mimics

Mouse peritoneal neutrophils were preincubated with 10 DPI or 10  $\mu$ mol/L 4-ABH at 37°C for 15 min. *S. aureus*, which were cultured in SCD broth until the mid-log phase growth, were treated with 10% pooled mouse serum for effective neutrophilic endocytosis of *S. aureus*. Bacteria were added to neutrophils at the bacteria-to-neutrophil ratio of 10:1 ( $1 \times 10^6$  neutrophils/mL), and incubation proceeded at 37°C with reciprocal shaking at 0.5 Hz. After 30 min of incubation, non-phagocytosed bacteria were removed by swing-out centrifugation (at  $110 \times g$ , 4 min) and neutrophils were washed three times with PBS (+) containing 10  $\mu$ mol/L DPI. Phagocytosed bacteria were precipitated with neutrophils, but non-phagocytosed bacteria were retained in the supernatant. Neutrophils that ingested the bacteria were incubated at 37°C for 30 min with shaking, with increasing concentrations of PEG-DAO (10, 50 and 100  $\mu$ M) in the presence of 10 mmol/L D-Ala and PBS (+) containing 10  $\mu$ mol/L DPI. Samples were diluted with 0.2% Tween-20, incubated at room temperature for five minutes to release phagocytosed bacteria, and vortexed vigorously, after which duplicate 100- $\mu$ L aliquots were plated on 15 mL plates of SCD agar gel followed by overnight culture at 37°C. The numbers of viable bacteria were counted as described above.

## Results

### Bacteriostatic activity of PEG-DAO

We first examined the bacteriostatic activity of PEG-DAO against *S. aureus*. In the presence of 10 mmol/L D-Ala,

PEG-DAO showed bacteriostatic activity in a dose-dependent manner (Figure 1a). Different concentrations of D-Ala also demonstrated dose-dependent activity (Figure 1b). Bacteriostatic activity was not observed with treatment of PEG-DAO and L-Ala (Figure 1a). Adding 1 mg/mL catalase (5000–15,000 U/mL) to samples with PEG-DAO and D-Ala nullified the bacteriostatic activity of PEG-DAO (Figure 1c).

**PEG-DAO restored antibacterial activity of NADPH oxidase-deficient mouse neutrophils**

As H<sub>2</sub>O<sub>2</sub> is a highly cell permeable oxidant, we examined H<sub>2</sub>O<sub>2</sub> generated by PEG-DAO plus D-Ala in the medium to determine whether H<sub>2</sub>O<sub>2</sub> could penetrate cell membranes and enter the cells. H<sub>2</sub>O<sub>2</sub> treatment increased oxidative stress inside neutrophils, as shown by analysis using fluorescence flow cytometry in the presence of the fluorescent reactive oxygen species probe dichlorofluorescein diacetate (DCFH-DA) (Figure 2a). In the presence of 10 mmol/L D-Ala, treatment with PEG-DAO increased the intracellular H<sub>2</sub>O<sub>2</sub> concentration in a dose-dependent manner as judged by this fluorescent probe (Figures 2b and c). However, PEG-DAO alone did not induce oxidative stress (data not shown). To mimic defective CGD neutrophils, mouse peritoneal neutrophils were treated with 10 μmol/L

DPI to inhibit NADPH oxidase. DPI treatment increased the numbers of viable bacteria inside the treated neutrophils, as seen by the colony forming assay (Figure 2d). However, PEG-DAO treatment in the presence of 10 mmol/L D-Ala restored bactericidal activity of DPI-treated defective neutrophils; the number of viable bacteria inside neutrophils almost recovered to the normal, non-CGD control. No enhancement of antibacterial activity by PEG-DAO in normal neutrophils was observed (Figure 2d).

**PEG-DAO induced MPO-dependent bactericidal activity of CGD-equivalent mouse neutrophils**

Consistent with the results shown in Figure 2, the bactericidal activity of mouse peritoneal neutrophils, which had been pretreated with DPI and thus had no NADPH oxidase activity, was restored by adding PEG-DAO and D-Ala (Figure 3). Treatment with 4-ABH, a specific inhibitor of MPO, clearly suppressed the bactericidal activity of normal mouse neutrophils. An interesting finding was the significant suppression of bactericidal activity of neutrophils by 4-ABH treatment, even with added PEG-DAO and D-Ala. This result demonstrates the important role of MPO in PEG-DAO-mediated bacterial killing (Figure 3).

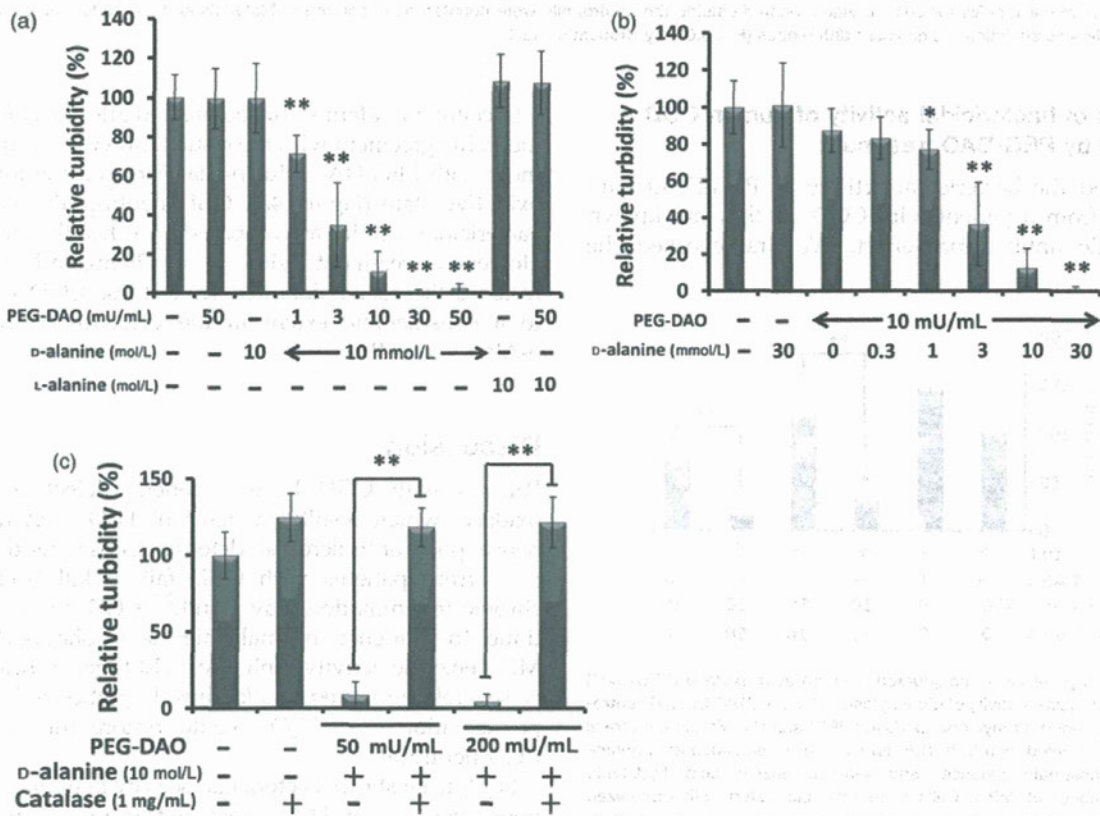
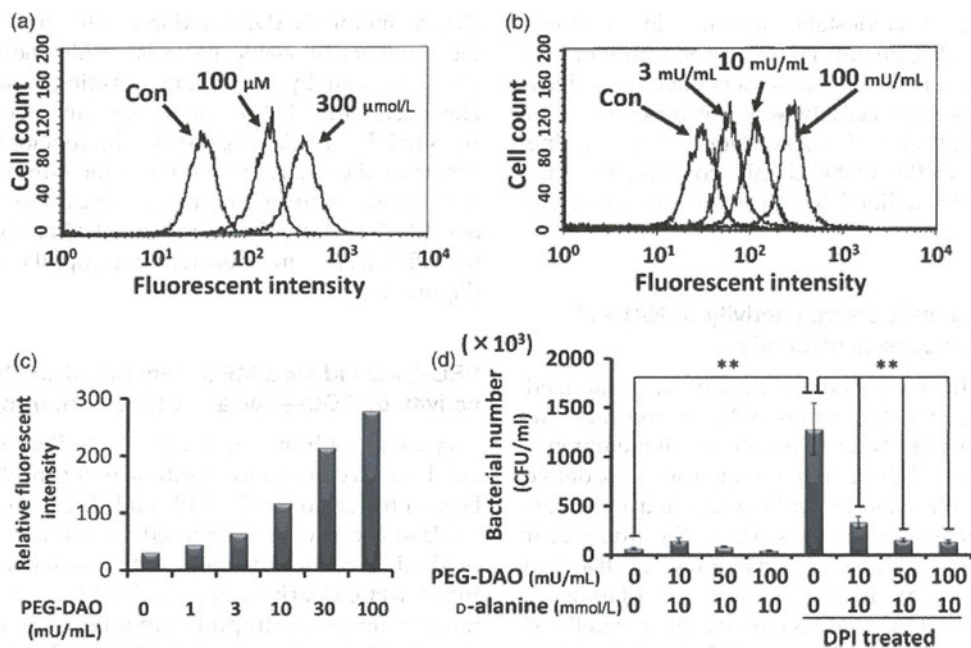


Figure 1 Bacteriostatic activity of polyethylene glycol-conjugated D-amino acid oxidase (PEG-DAO) against *Staphylococcus aureus*. (a) Increasing concentrations of PEG-DAO in the presence of 10 mmol/L D-Ala or (b) increasing concentrations of D-Ala in the presence of 10 mU/mL PEG-DAO were incubated with *S. aureus* bacteria (1 × 10<sup>6</sup> CFU/mL) for five hours, after which turbidity at 570 nm was measured. (c) *S. aureus* bacteria (1 × 10<sup>6</sup> CFU/mL) were incubated for five hours with PEG-DAO plus D-Ala with or without 1 mg/mL bovine catalase, and after which turbidity at 570 nm was measured. \*\* and \* indicate statistically significant differences (P < 0.01) and (P < 0.05), respectively, by Student's t-test. Values are means ± SD (n = 12)



**Figure 2** Increase in intracellular hydrogen peroxide ( $H_2O_2$ ) by means of treatment with polyethylene glycol-conjugated D-amino acid oxidase (PEG-DAO) plus D-Ala and restoration of bactericidal activity of chronic granulomatous disease-like neutrophils. Mouse peritoneal neutrophils were pretreated with  $10 \mu\text{mol/L}$  dichlorofluorescein diacetate, a fluorescent molecular probe for  $H_2O_2$ , and were then incubated with (a) increasing concentrations of  $H_2O_2$  or (b) increasing concentrations of PEG-DAO (1–100 mU/mL) plus a fixed amount of  $10 \text{ mmol/L}$  D-Ala, followed by incubation for 30 min at room temperature. The fluorescence intensity of neutrophils was measured by means of a flow cytometer. (c) Normalized fluorescence intensity of cells in (b) representing intracellular reactive oxygen species. (d) Mouse peritoneal neutrophils were pretreated with  $10 \mu\text{mol/L}$  diphenylene iodonium (DPI) and were then incubated with opsonized *Staphylococcus aureus* to allow phagocytosis for 30 min. After removal of non-phagocytosed bacteria in the supernatant, neutrophils were treated with PEG-DAO plus  $10 \text{ mmol/L}$  D-Ala for 30 min. Viable bacteria inside the neutrophils were counted as described in Materials and methods. Values are means  $\pm$  SE ( $n = 4$ ). \*\*Indicates statistically significant differences ( $P < 0.01$ ) by Student's *t*-test

### Restoration of bactericidal activity of human CGD neutrophils by PEG-DAO treatment

We examined the bactericidal activity of PEG-DAO with neutrophils from a patient with CGD, as they are known to have little antibacterial effect. We first checked the

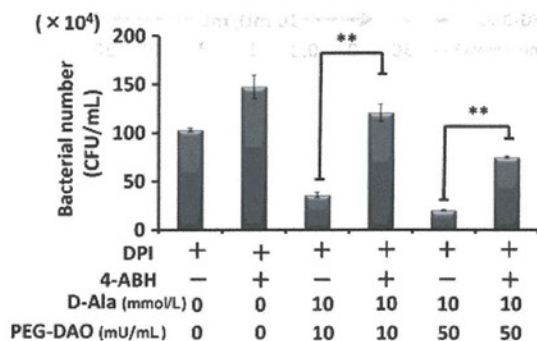


**Figure 3** Polyethylene glycol-conjugated D-amino acid oxidase (PEG-DAO) restored the bactericidal activity of diphenylene iodonium (DPI)-treated neutrophils, which depended on myeloperoxidase (MPO) activity. Mouse peritoneal neutrophils were treated with both DPI, an inhibitor of nicotinamide adenine dinucleotide phosphate oxidase, and 4-aminobenzoic acid hydrazide (4-ABH), an inhibitor of MPO. Cells were then incubated with opsonized *Staphylococcus aureus* to allow phagocytosis. After removal of non-phagocytosed bacteria, neutrophils were treated with PEG-DAO for 30 min. The number of viable bacteria was derived from the count of colonies on agar plates, as described in Materials and methods. Values are means  $\pm$  SE ( $n = 4$ ). \*\*Indicates statistically significant differences ( $P < 0.01$ ) by Student's *t*-test

intracellular oxidant status before and after PEG-DAO treatment. In agreement with the results shown in Figure 2, treatment with PEG-DAO plus D-Ala increased the intracellular oxidative state (Figure 4a). CGD neutrophils showed less bactericidal activity as compared with healthy neutrophils. However, treatment with 10 or 30 mU/mL PEG-DAO restored the bactericidal activity of these CGD neutrophils to a considerable extent in the presence of  $10 \text{ mmol/L}$  D-Ala (Figure 4b).

### Discussion

Patients with CGD have a genetic defect in NADPH oxidase, which results in deficient  $H_2O_2$  generation and hence poor antimicrobial defense. Consequently, neutrophils from patients with CGD fail to kill bacteria, and chronic inflammation may result.<sup>2,3</sup> CGD neutrophils continue to evidence normal migration, phagocytosis and MPO enzyme activity; only their  $H_2O_2$ -generating capacity is severely impaired.<sup>10</sup> We thus hypothesized that supplementation with  $H_2O_2$  would restore this function of CGD neutrophils.

$H_2O_2$  itself shows bactericidal activity *in vitro*, but intravenous injection of  $H_2O_2$  does not result in antibacterial activity against bacteria *in vivo* because of the presence of excess catalase in the systemic circulation.<sup>11</sup> In other words, circulating  $H_2O_2$  *in vivo* is rapidly cleared by catalase, so no  $H_2O_2$  is available for targeting to infected or



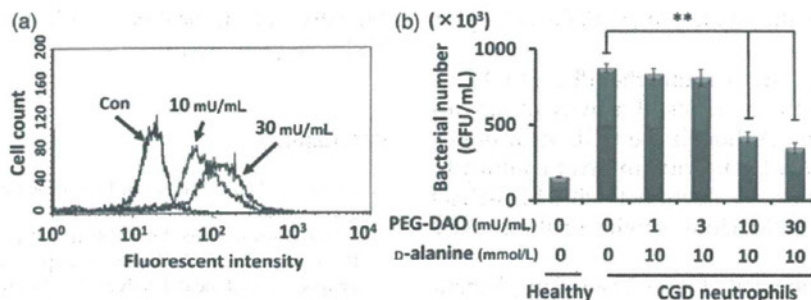


**Figure 4** Restoration of bactericidal function of human chronic granulomatous disease (CGD) neutrophils by polyethylene glycol-conjugated D-amino acid oxidase (PEG-DAO) treatment. (a) Human CGD neutrophils were pretreated with 10  $\mu$ mol/L dichlorofluorescein diacetate, an intracellular marker of oxystress, and were then incubated with PEG-DAO (10 or 30 mU/mL) and 10 mmol/L D-Ala for 30 min at room temperature. The fluorescence intensity of the neutrophils was measured by using a fluorescence flow cytometer. (b) CGD neutrophils were incubated with *Staphylococcus aureus* to allow phagocytosis. After removal of the non-phagocytosed *S. aureus* by centrifugation, neutrophils were treated with PEG-DAO and D-Ala for 30 min followed by incubation with 0.2% Tween-20 to liberate bacteria from the neutrophils. Serial dilutions of bacteria were then mixed with Trypticase soy agar in Petri dishes and incubated overnight at 37°C, and bacterial colonies was counted. Values are means  $\pm$  SE ( $n = 3$ ). \*\*Indicates statistically significant differences ( $P < 0.01$ ) by Student's *t*-test

inflamed sites. Furthermore, H<sub>2</sub>O<sub>2</sub> may harm mammalian cells that have no catalase or other antioxidants.<sup>11</sup> Thus, new strategies to deliver the H<sub>2</sub>O<sub>2</sub> to the target site are required, which may provide a new strategy of H<sub>2</sub>O<sub>2</sub>-dependent treatment of infection and cancer.

To achieve the delivery of H<sub>2</sub>O<sub>2</sub> to an infected or inflamed site, we prepared PEG-DAO which retained a degree of H<sub>2</sub>O<sub>2</sub>-generating activity that was comparable with that of native DAO.<sup>5,7</sup> Also, DAO derived from a porcine source can be used in humans, because PEGylation reduces the antigenicity of this enzyme. PEG-DAO accumulates preferentially in tumor tissue because of the EPR effect, the mechanism of which is based on the highly enhanced extravasation of macromolecules in the tumor and inflamed tissues. In addition, impaired lymphatic clearance of such macromolecules from interstitial space makes this effect more distinct. This increased vascular permeability is induced partly by overproduction of inflammatory vascular mediators such as bradykinin, nitric oxide and many others.<sup>2,8</sup>

The concentrations of D-amino acids, which are substrates of PEG-DAO, are extremely low in mammalian blood plasma, so H<sub>2</sub>O<sub>2</sub> generation by PEG-DAO alone in systemic circulation is quite limited. However, we can induce H<sub>2</sub>O<sub>2</sub> generation with an intravenous injection of D-amino acids. PEG-DAO at first accumulates predominantly at the inflamed site because of the EPR effect. After several hours of PEG-DAO infusion via an intravenous route allowing PEG-DAO to accumulate more selectively at the disease site, at that time, the PEG-DAO concentration in blood is very low, and D-amino acid is infused subsequently via the intravenous route. Thus, PEG-DAO is preferable for delivery of H<sub>2</sub>O<sub>2</sub> to the inflamed sites or cancer tissue, and avoids systemic generation of H<sub>2</sub>O<sub>2</sub>.<sup>6</sup>

PEG-DAO plus D-Ala, as mediated by H<sub>2</sub>O<sub>2</sub>, showed bacteriostatic activity against *S. aureus* in a dose-dependent manner via production of H<sub>2</sub>O<sub>2</sub> (Figure 1). These results indicate that PEG-DAO can serve as an antibacterial agent if it is selectively delivered to an infected site. This delivery became a possibility as a result of the prolonged plasma half-life of PEG-DAO and the EPR effect.

When PEG-DAO plus D-Ala was supplied to NADPH oxidase-deficient neutrophils, it increased the amount of

H<sub>2</sub>O<sub>2</sub> inside the cells (Figures 2 and 4). The fluorescent oxystress probe DCFH-DA, which effectively enters neutrophils, contains a diacetate group that is quickly hydrolyzed, so DCFH-DA becomes reactive to H<sub>2</sub>O<sub>2</sub> and then fluorescent.<sup>12</sup> The higher fluorescence intensity of DCFH-DA thus indicates a higher oxidative state inside cells, but does not reflect the oxidative state outside cells. As expected, PEG-DAO treatment or H<sub>2</sub>O<sub>2</sub> treatment increased the intracellular level of H<sub>2</sub>O<sub>2</sub> in a dose-dependent manner (Figure 2a). Furthermore, in the presence of D-Ala, addition of PEG-DAO also increased the amount of intracellular H<sub>2</sub>O<sub>2</sub> in a dose-dependent manner (Figures 2a and b). These results clearly indicate that PEG-DAO treatment can supply exogenous H<sub>2</sub>O<sub>2</sub> efficiently to neutrophils and that this restored level of intracellular H<sub>2</sub>O<sub>2</sub>, as H<sub>2</sub>O<sub>2</sub> is converted to the hypochlorite ion by MPO, would facilitate potent bactericidal activity of neutrophils from a CGD patient.

We also examined whether PEG-DAO treatment would restore the bactericidal activity of CGD-like neutrophils. We prepared neutrophil mimics, which were similar to neutrophils in patients with CGD, by pretreatment with 10  $\mu$ mol/L DPI, which achieves its effects by inhibiting NADPH oxidase and thus suppressing H<sub>2</sub>O<sub>2</sub> generation.<sup>13</sup> In this experiment, we used PEG-DAO plus D-Ala and examined the effect of this treatment on phagocytosed bacteria. We observed a significant increase in the number of viable bacteria inside these neutrophils after DPI treatment (Figure 2d). In this setting, the bactericidal activity of DPI-treated neutrophils was similar to that of neutrophils from a CGD patient. However, PEG-DAO treatment of DPI-treated neutrophils greatly suppressed the number of viable bacteria inside neutrophils, almost to the number in healthy neutrophils (Figure 2d).

Most MPO exists in vacuoles in neutrophils,<sup>14</sup> and MPO oxidizes the chloride ion, with H<sub>2</sub>O<sub>2</sub>, to produce hypochlorous acid, one of the most potent bactericidal molecules in biological systems. We therefore hypothesized that restoration of bactericidal activity of DPI-treated neutrophils by treatment of PEG-DAO and D-Ala was mediated by the function of MPO. Consistent with our hypothesis, 4-ABH, an MPO inhibitor, suppressed the bactericidal activity of

the neutrophils, even in the treatment of PEG-DAO plus D-Ala (Figure 3).

As a more important result, we found that PEG-DAO plus D-Ala treatment restored the bactericidal activity of neutrophils from a CGD patient. Although the CGD neutrophils showed decreased bactericidal activity, in great contrast to healthy neutrophils (Figure 4), treatment with PEG-DAO plus D-Ala restored the bactericidal activity of these CGD neutrophils (Figure 4).

Our results thus demonstrated that H<sub>2</sub>O<sub>2</sub> supplementation via PEG-DAO plus D-Ala would protect against bacterial infection. In our experiments, we used porcine DAO to prepare PEG-DAO. For porcine DAO, the K<sub>cat</sub> and K<sub>m</sub> values for D-proline are 43.3 s<sup>-1</sup> and 2 mmol/L, respectively, whereas the corresponding values for D-Ala are 6.4 s<sup>-1</sup> and 3.1 mmol/L.<sup>15</sup> Thus, using D-proline may be preferable to using D-Ala to treat CGD neutrophils, although this issue requires additional investigation. Furthermore, H<sub>2</sub>O<sub>2</sub> can enter the cytosol of neutrophils and be converted to hypochlorous acid by MPO. These observations suggest that H<sub>2</sub>O<sub>2</sub> supplementation via enzymatic action may become a plausible approach for treatment of patients with CGD. Less useful therapeutic strategies for CGD exist as yet, despite the great advances in the development of antimicrobial agents. The previously reported pharmacokinetics of PEG-DAO indicated an effective targeting ability to solid tumors as a result of the EPR effect. Bacterial components such as bacterial proteases and endotoxin facilitate the vascular permeability, and thus leakage of blood components such as albumin from circulating blood. Consequently, these macromolecules will accumulate at the infected or inflamed site.<sup>16,17</sup> Although the accumulation property of macromolecular proteins at the tumor and inflamed tissue is similar, accumulation of PEG-DAO at the inflamed tissue in the CGD mouse model of human patients is yet to be determined. PEG-DAO pharmacokinetics may be similarly beneficial for targeting to the inflamed granuloma tissue in patients with CGD, although more studies are needed to confirm this possibility.

**Author contributions:** All authors participated in the design, interpretation of the studies, analysis of the data and review of the manuscript. HNa conducted the experiments and wrote the manuscript with HM; TM and HNu supplied the critical sample; and JF and HM discussed the content constructively for the experiments and revised the manuscript.

#### ACKNOWLEDGEMENTS

The use of blood samples from a patient with CGD was approved by the Institutional Review Board of University of Miyazaki, Japan. This work was supported by Grant-in-Aid for Scientific Research 21791016 from the

Ministry of Education, Culture, Sports, Science and Technology of Japan.

#### REFERENCES

- Hohn DC, Lehrer RI. NADPH oxidase deficiency in X-linked chronic granulomatous disease. *J Clin Invest* 1975;55:707-13
- Johnston RB Jr, Keele BB Jr, Misra HP, Lehmeier JE, Webb LS, Baehner RL, Rajagopalan KV. The role of superoxide anion generation in phagocytic bactericidal activity. Studies with normal and chronic granulomatous disease leukocytes. *J Clin Invest* 1975;55:1357-72
- Repine JE, Clawson CC. Quantitative measurement of the bactericidal capability of neutrophils from patients and carriers of chronic granulomatous disease. *J Lab Clin Med* 1977;90:522-8
- Burton K. The stabilization of D-amino acid oxidase by flavin-adenine dinucleotide, substrates and competitive inhibitors. *Biochem J* 1951;48:458-67
- Mosebach KO. [Mechanism of action of some factors affecting D-amino acid oxidase. III. Reactions and significance of nascent hydrogen peroxides.]. *Hoppe Seylers Z Physiol Chem* 1957;309:206-18
- Fang J, Sawa T, Akaike T, Maeda H. Tumor-targeted delivery of polyethylene glycol-conjugated D-amino acid oxidase for antitumor therapy via enzymatic generation of hydrogen peroxide. *Cancer Res* 2002;62:3138-43
- Fang J, Deng D, Nakamura H, Akuta T, Qin H, Iyer AK, Greish K, Maeda H. Oxystress inducing antitumor therapeutics via tumor-targeted delivery of PEG-conjugated D-amino acid oxidase. *Int J Cancer J Int Cancer* 2008;122:1135-44
- Matsumura Y, Maeda H. A new concept for macromolecular therapeutics in cancer chemotherapy: mechanism of tumoritropic accumulation of proteins and the antitumor agent smancs. *Cancer Res* 1986;46:6387-92
- Fang J, Nakamura H, Maeda H. The EPR effect: unique features of tumor blood vessels for drug delivery, factors involved, and limitations and augmentation of the effect. *Adv Drug Deliv Rev* 2011;63:136-51
- Gougerot-Pocidal MA, Elbim C, Dang PM, El Benna J. [Primary immune deficiencies in neutrophil functioning]. *Presse Med* 2006;35:871-8
- Shenep JL, Stokes DC, Hughes WT. Lack of antibacterial activity after intravenous hydrogen peroxide infusion in experimental *Escherichia coli* sepsis. *Infect Immun* 1985;48:607-10
- Lebel CP, Bondy SC. Sensitive and rapid quantitation of oxygen reactive species formation in rat synaptosomes. *Neurochem Int* 1990;17:435-40
- Ellis JA, Mayer SJ, Jones OT. The effect of the NADPH oxidase inhibitor diphenyleneiodonium on aerobic and anaerobic microbicidal activities of human neutrophils. *Biochem J* 1988;251:887-91
- Rosen H, Crowley JR, Heinecke JW. Human neutrophils use the myeloperoxidase-hydrogen peroxide-chloride system to chlorinate but not nitrate bacterial proteins during phagocytosis. *J Biol Chem* 2002;277:30463-8
- Molla G, Sacchi S, Bernasconi M, Pilone MS, Fukui K, Polegioni L. Characterization of human D-amino acid oxidase. *FEBS Lett* 2006;580:2358-64
- Xing J, Moldobaeva N, Birukova AA. Atrial natriuretic peptide protects against *Staphylococcus aureus*-induced lung injury and endothelial barrier dysfunction. *J Appl Physiol* 2011;110:213-24
- Kamata R, Yamamoto T, Matsumoto K, Maeda H. A serratal protease causes vascular permeability reaction by activation of the Hageman factor-dependent pathway in guinea pigs. *Infect Immun* 1985;48:747-53

(Received October 28, 2011, Accepted February 16, 2012)